DOI: 10.1002/zaac.201200341

Two Zinc(II) Coordination Polymers Based on the Ligand 1,4-Bis[(2-methyl-imidazol-1-yl)methyl]benzene: Syntheses, Crystal Structures and Properties

Jing-Tao Shi,[a] Chun-Sheng Zhou,[a,b] Yong-Liang Liu,[a] Zhi-Guo Fang,[a] Rui-Li Zhao,[a] Li-Li Xu,[a] and Ke-Fen Yue*[a]

Keywords: Bisimidazole ligand; Interpenetration; Zinc; Coordination polymers

Abstract. Two coordination polymers (CPs), $\{[Zn_2(BMB)(5\text{-}AIPA)_2]\cdot 2H_2O\}_n$(**1**) and $[Zn(BMB)(5\text{-}NIPA)]_n$(**2**) {BMB = 1,4-bis[(2-methyl-imidazol-1-yl)methyl]benzene, 5-AIPA = 5-aminoisophthalic acid, 5-NIPA = 5-nitroisophthalic acid}, were synthesized under hydrothermal conditions. Compound **1** displays a 2D double-layer structure, which is packed into a 3D supramolecule by interlayer hydrogen bonds and π–π stacking interactions. Compound **2** displays a threefold interpenetrating 3D network, which is composed of left-handed helical chains and two types of *meso*-helical chains along different directions.

Introduction

The rational synthesis of hybrid coordination polymers (CPs) has attracted immense attention because of their various structural topologies and potential application in many areas such as molecular magnetism, catalysis, and gas absorbents.[1–6] The multiple structures and unique properties of coordination polymers have relation to the organic and inorganic components.[7–11] Flexible bisimidazole ligands as good candidates for the formation of novel CPs easily form interpenetrating structures and helical modes, since they are able to twist and rotate freely to adopt a suitable conformation in constructing process [12–16].

Recently, bisimidazole ligands have attracted much attention in the field of crystal engineering. Some coordination polymers contained bisimidazole ligands have been documented in the literatures.[17,18] However, CPs constructed by BMB has not been well studied to date.[19,20] In our previous work, we have designed and synthesized systematically topologically interesting coordination structures based on flexible bisimidazole ligands, 1,4-bis(2-methyl-imidazol-1-yl)butane and 1,6-bis(2-methyl-imidazole-1-yl)hexane.[21–23] To expand our investigations in this field, we select the other bisimidazole ligand, 1,4-bis[(2-methyl-imidazol-1-yl)methyl]benzene (BMB). It has shown the ability to produce unique *meso*-helical features because of two freely rotating $–CH_2–$ groups and a rigid spacer of phenyl ring.[24] The *meso*-helical chains contain both left- and right-handed helical loops in each chain like a lemniscate, and display a "∞" shape.[25]

Herein, we report on two CPs, $\{[Zn_2(BMB)(5\text{-}AIPA)_2]\cdot 2H_2O\}_n$(**1**) and $[Zn(BMB)(5\text{-}NIPA)]_n$(**2**), which were obtained under hydrothermal conditions and exhibit interesting 2D double-layer and 3D threefold interpenetrating topologies, respectively. They were characterized by elemental analysis, IR spectroscopy, and X-ray crystallography. Additionally, the thermal and photoluminescence properties are presented.

Results and Discussion

Description of Crystal Structures

Structure of $\{[Zn_2(BMB)(5\text{-}AIPA)_2]\cdot 2H_2O\}_n$ **(1)**

X-ray diffraction analysis revealed that compound **1** crystallizes in the monoclinic space group $P2_1/c$ (Table 1). The asymmetric unit of **1** consists of one Zn^{II} ion, a half of a BMB, and one 5-AIPA molecule (Figure 1). The central Zn^{II} atom has a slightly distorted trigonal bipyramidal arrangement and is surrounded by one nitrogen atom (N1) from the BMB molecule, two oxygen atoms, and one nitrogen atom (N3) from different 5-AIPA ligands. The Zn–O bond lengths are 1.948(2) and 1.999(2) Å. The Zn–N1 bond length is 2.008(2) Å and the Zn–N3 bond length is 2.067(2) Å. Selected bond lengths and angles are given in Table 2. Thus, each 5-AIPA links three Zn^{II} ions to form an infinite 2D layer. The BMB ligands are attached to the two layers to construct double-layer as shown in Figure 2. The double-layers are further connected together by

---

* Prof. Dr. K.-F. Yue
Fax: +86-29-88302604
E-Mail: ykflyy@nwu.edu.cn
[a] Key Laboratory of Synthetic and Natural Functional Molecule Chemistry of the Ministry of Education
Shaanxi Key Laboratory of Physico-Inorganic Chemistry
College of Chemistry and Materials Science, Northwest University
Xi′an 710069, P. R. China
[b] Department of Chemistry
Shang Luo University
Shang Luo 726000, P. R. China

Supporting information for this article is available on the WWW under **http://dx.doi.org/10.1002/zaac.201200341** or from the author.

Table 1. Crystal data and structure refinements for compounds **1** and **2**.

	1	**2**
Molecular formula	$C_{16}H_{16}N_3O_5Zn$	$C_{24}H_{21}N_5O_6Zn$
Fw	395.69	540.83
Temperature	296(2)	150
Crystal system	monoclinic	Monoclinic
Space group	$P2_1/c$	$P2/c$
a /Å	12.7129(10)	17.795(6)
b /Å	7.8758(6)	7.305(2)
c /Å	15.9859(13)	24.447(6)
α /°	90	90
β /°	91.3320(10)	133.221(15)
γ /°	90	90
V /Å^3	1600.1(2)	2315.8(12)
Z	4	4
ρ /g·cm^{-3}	1.642	1.551
F(000)	812	1112
Reflections collected / unique	7764 / 2846	13684 / 5577
[R(int)]	[0.0222]	[0.0649]
Goodness-of-fit on F^2	1.11	1.03
Final R indices [$I > 2\sigma(I)$]	$R_1 = 0.0268$, $wR_2 = 0.0803$	$R_1 = 0.0568$, $wR_2 = 0.1393$
R indices (all data)	$R_1 = 0.0351$, $wR_2 = 0.0953$	$R_1 = 0.1063$, $wR_2 = 0.1765$

two kinds of hydrogen bonding interactions between the amino group (–N3) and carboxylate oxygen atoms (N3···O1, 3.049 Å, N3···O2, 3.153 Å) (Figure 3a,b). Meanwhile, there are strong π–π stacking interactions between the benzene rings of interlayers with a face-to-face distance of 3.368 Å (Figure 3a,c). Besides, O–H···O hydrogen bonds (O1W···O2, 2.918 Å; O1W···O3, 2.995 Å) exist between protonated carboxylate groups and uncoordinated water molecules (Table S1; Supporting Information). Finally, the 2D double-layers are further extended into a 3D supramolecular architecture through hydrogen bonds and π–π stacking interactions.

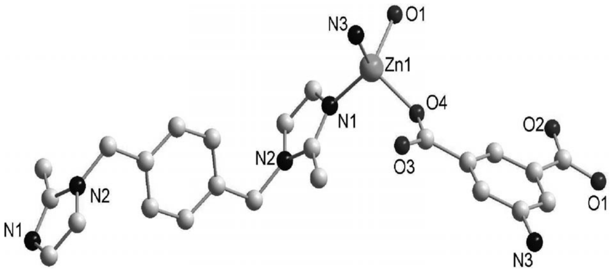

Figure 1. Coordination environment of the Zn^{II} ion in **1**.

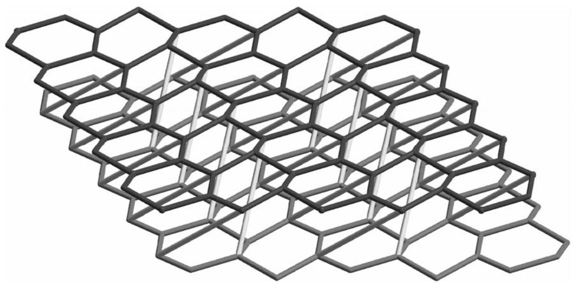

Figure 2. Schematic representation of the 2D double-layer of compound **1**.

Structure of [Zn(BMB)(5-NIPA)]$_n$ (2)

The asymmetric unit of **2** contains two half Zn^{II} atoms, one BMB, one 5-NIPA ligand and belongs to the monoclinic space group *P*2/*c* (Table 1). As illustrated in Figure 4, the two Zn^{II} atoms exhibit similar coordination arrangements. Zn1^{II} is four-coordinate with two oxygen atoms (O1) of two 5-NIPA ligands besides two nitrogen atoms (N3) from two BMB ligands, and Zn2^{II} is coordinated by two O3 and two N1 atoms. The Zn–N and Zn–O bond lengths are all within the reasonable ranges. Selected bond lengths and angles are given in Table 2. In **2**, Zn1 and Zn2 are bridged by BMB ligands to form two similar 1D *meso*-helical chains, namely (Zn1–BMB)$_n$ and (Zn2–BMB)$_n$

Table 2. Selected bond lengths /Å and angles /° for **1** and **2**.

1^a			
Zn(1)–O(4)#1	1.9478(17)	Zn(1)–O(1)	1.9991(16)
Zn(1)–N(1)	2.008(2)	Zn(1)–N(3)#2	2.0670(18)
O(4)–Zn(1)#3	1.9478(17)	N(3)–Zn(1)#4	2.0670(18)
O(4)#1–Zn(1)–O(1)	106.10(7)	O(4)#1–Zn(1)–N(1)	105.75(8)
O(1)–Zn(1)–N(1)	108.49(8)	O(4)#1–Zn(1)–N(3)#2	108.08(7)
O(1)–Zn(1)–N(3)#2	105.85(7)	N(1)–Zn(1)–N(3)#2	121.66(8)
2^b			
Zn(1)–O(1)	1.959(5)	Zn(1)–O(1)#1	1.959(5)
Zn(1)–N(3)#1	2.022(5)	Zn(1)–N(3)	2.022(5)
Zn(2)–O(3)#2	1.968(4)	Zn(2)–O(3)	1.968(4)
Zn(2)–N(1)	2.052(5)	Zn(2)–N(1)#2	2.052(5)
O(1)–Zn(1)–O(1)#1	121.0(3)	O(1)–Zn(1)–N(3)#1	123.4(2)
O(1)#1–Zn(1)–N(3)#1	94.2(2)	O(1)–Zn(1)–N(3)	94.2(2)
O(1)#1–Zn(1)–N(3)	123.4(2)	N(3)#1–Zn(1)–N(3)	101.5(3)
O(3)#2–Zn(2)–O(3)	122.9(3)	O(3)#2–Zn(2)–N(1)	106.0(2)
O(3)–Zn(2)–N(1)	111.73(19)	O(3)#2–Zn(2)–N(1)#2	111.73(19)
O(3)–Zn(2)–N(1)#2	106.0(2)	N(1)–Zn(2)–N(1)#2	95.1(3)

Symmetry transformations used to generate equivalent atoms: a: #1 *x*, –*y*+1/2, *z*+1/2; #2 *x*, *y*+1, *z*; #3 *x*, –*y*+1/2, *z*–1/2; #4 *x*, *y*–1, *z*; #5 –*x*, –*y*+2, –*z* b: #1 –*x*+1, *y*, –*z*+3/2; #2 –*x*+2, *y*, –*z*+3/2; #3 –*x*+2, –*y*, –*z*+1; #4 –*x*, –*y*+3, –*z*+1.

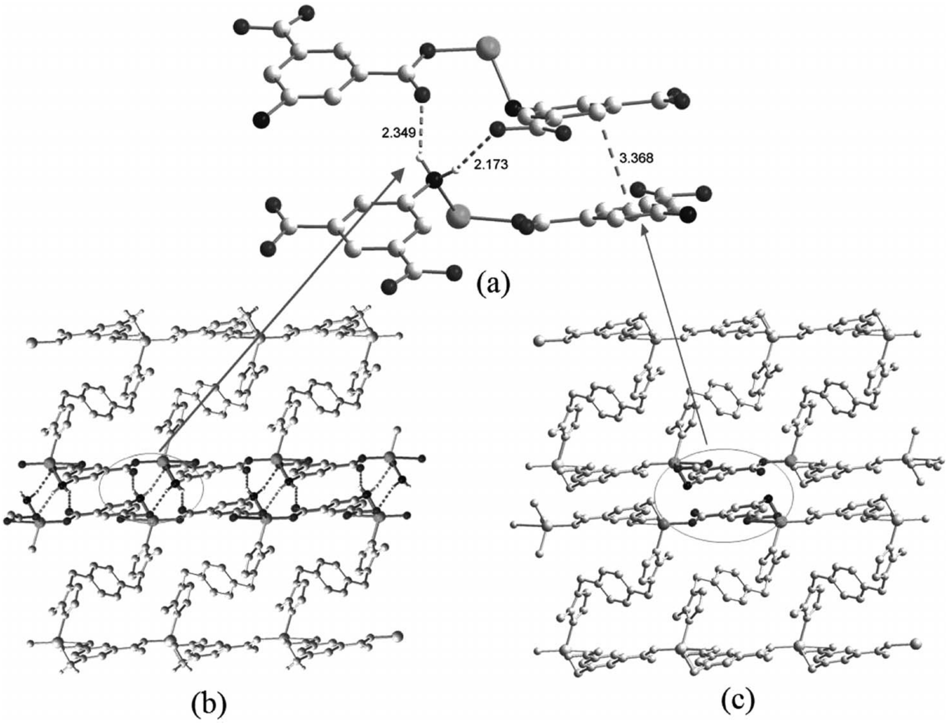

Figure 3. (a). Schematic representation of hydrogen bonding and π–π interactions between the double-layers in **1**. (b) Packing of the 3D framework by hydrogen bonds. (c) Packing diagram showing π–π interactions between the 5-AIPA molecules.

with a pitch of 25.85 and 24.35 Å respectively (Figure 5a). Each 5-NIPA ligand connects the atoms Zn1 and Zn2 in a monodentate coordination mode to form a 1D left-handed helical chain (Zn-5-NIPA)$_n$ (see Figure 5b). The (Zn1–BMB)$_n$, (Zn2–BMB)$_n$, and (Zn–5-NIPA)$_n$ helical chains are joined together to a 3D network (Figure 5c). Finally, the independent equivalent 3D frameworks give rise to a threefold interpenetrating net with the point symbol $6^5.8$ and the long symbol $6.6.6.6.6_2.8_3$, as seen in Figure 5d.

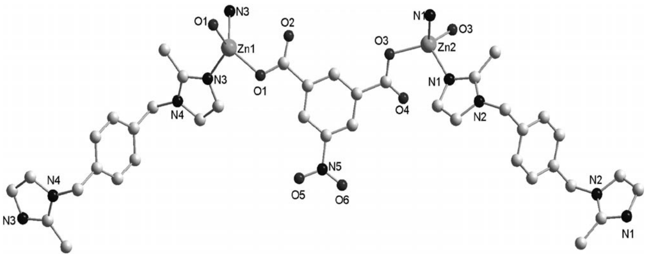

Figure 4. Coordination environment of the Zn^{II} ion in **2**.

Meanwhile, the atoms $Zn1^{II}$ and $Zn2^{II}$ are alternatingly linked via two types of BMB and 5-NIPA ligands extending into *meso*-helical chains, which can be described as (Zn1–N3···N3BMB–Zn1–NIPA–Zn2–N1···N1BMB–Zn2–NIPA–Zn1)$_n$ (Figure 6a). In the structure of 3D frameworks, the rigid benzene rings of BMB between three *meso*-helical chains form π–π interactions with an intercentroid distance of 3.703 Å (Figure 6b).

Photoluminescent Properties

The solid-state luminescent properties of the ligands as well as compounds **1**, and **2** were investigated at room temperature as shown in Figure 7. As previously reported,[26,27] the solid aromatic carboxylate ligands (5-AIPA, 5-NIPA) are nearly non-fluorescent in the range 400–600 nm, and the free co-ligand BMB shows a maximum emission band at 505 nm (λ_{ex} = 280 nm). The emission bands of **1**, 5-AIPA, and BMB are observed at 344, 439, and 505 nm, respectively. The emission bands of **2** and BMB are observed at 465 and 505 nm, respectively. The emission peaks of **1** and **2** are both blue-shifted compared to ligands. The weak luminescent properties of 5-NIPA and **2** may originate from the obvious decrease of the electron density of the ligand affected by electron-withdrawing nitryl group.[28] Since Zn^{2+} ion is difficult to oxidize or to reduce owing to its d^{10} configuration, these bands can probably be assigned to the (π–π*) intraligand fluorescent emission.[18,29–31]

Thermal Behaviors and PXRD Results

Thermogravimetric analysis for **1** shows a small weight loss of 5.35 % (calcd. 4.55 %) before 200 °C, due to the loss of two lattice water molecules. The decomposition of its coordination framework occurred during 445–535 °C, which can be attributed to the organic ligands released progressively. For **2**, the decomposition of the framework occurred when the temperature is above 365 °C (Figure S1, Supporting Information). The

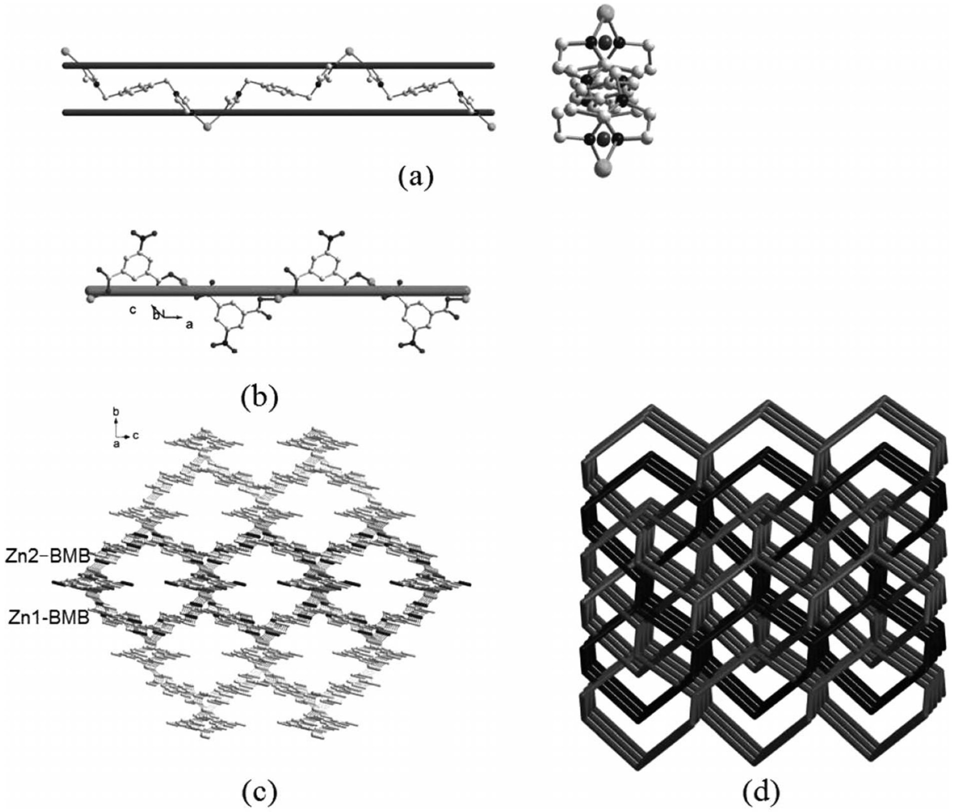

Figure 5. (a) View of the a type of Zn^{II} and BMB *meso*-helical chain and the "∞" shape of the *meso*-helices. (c) Left helical chain of Zn^{II} and 5-NIPA. (c) View of the 3D network accomplished by connecting three types of helical chains. (d) 3D threefold interpenetration topology in **2**.

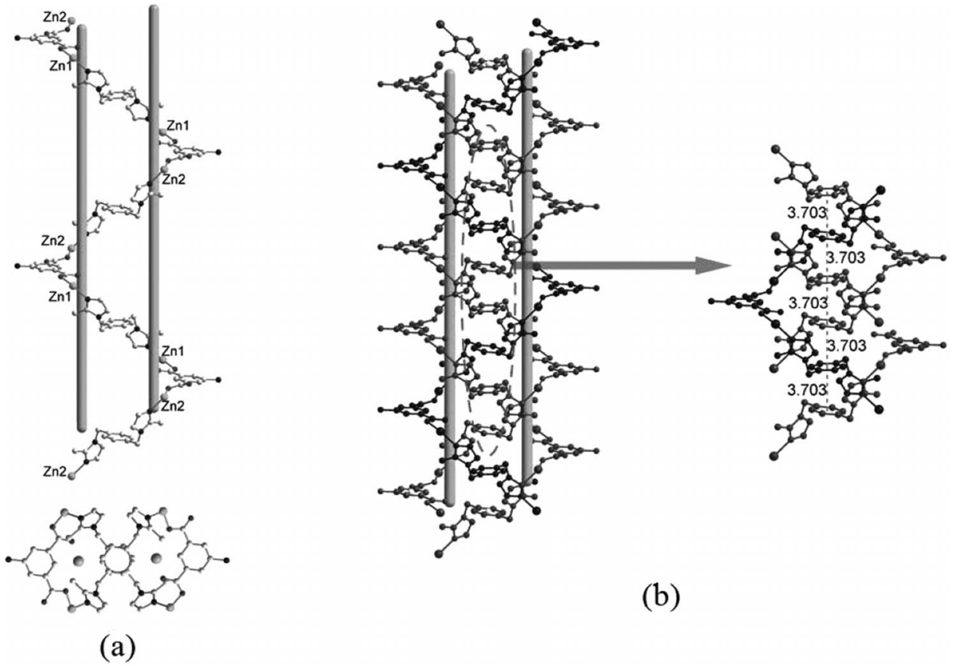

Figure 6. (a) View of the *meso*-helical chains of Zn^{II}, BMB, and NIPA $(Zn1–N3\cdots N3BMB–Zn1–NIPA–Zn2–N1\cdots N1BMB–Zn2–NIPA–Zn1)_n$ and the "∞" shape of the *meso*-helices along the *b* axis in **2**. (b) Three strands *meso*-helices $(Zn1–N3\cdots N3BMB–Zn1–NIPA–Zn2–N1\cdots N1BMB–Zn2–NIPA–Zn1)_n$ in threefold interpenetration framework and π–π interactions between 3D networks.

PXRD experiments for **1** and **2** were carried out to confirm whether the crystal structures are truly representative of the bulk materials. The experimental and computer-simulated patterns of the corresponding complexes are shown in Figure S2. We can see that the synthesized bulk materials and the measured single crystals are the same.

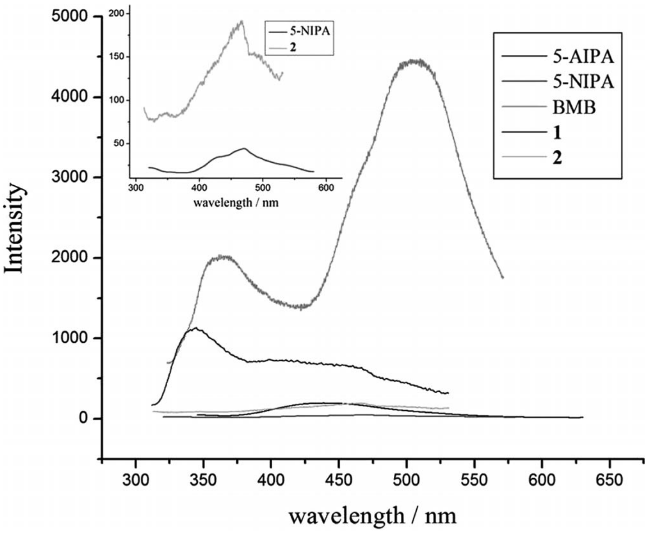

Figure 7. Solid-state photoluminescent spectra at room temperature.

Conclusions

Two novel CPs based on co-ligand BMB and dicarboxylate acid were synthesized under hydrothermal conditions. The co-ligand BMB could bend and rotate to construct novel CPs as a potential building block. The 2D double-layer of **1** is packed by interlayer hydrogen bonds and π–π stacking interactions to extend to a 3D supramolecule. Compound **2** generates a threefold interpenetrating 3D net containing left-handed helical chains and two types of *meso*-helical chains along different directions.

Experimental Section

Materials and Physical Measurements: All chemicals were of reagent grade and used without further purification. IR spectra using KBr pellets were recorded with a FT-IR 170 SX (Nicolet) spectrophotometer (4000–400 cm^{-1} region). Elemental analyses of C, H, and N were determined with a Perkin-Elmer 240C automatic analyzer. The TG-DTA measurements were carried out with a NETZSCH TG 209 thermal analyzer from room temperature to 900 °C in a nitrogen atmosphere with a heating rate of 10 K·min^{-1}. Fluorescence spectra were measured with a Hitachi F-7000 fluorescence spectrophotometer at room temperature. Single crystal X-ray data were measured with a Bruker SMART APEX CCD diffractometer using graphite monochromated Mo-K_α radiation (λ = 0.71073 Å) at 296 K for **1** and at 150 K for **2**. An empirical absorption correction was applied to the collected reflections with SADABS program. The structures were solved by direct methods and refined on F^2 by full-matrix least-squares methods using the SHELX-97 program package.[32] All non-hydrogen atoms were refined anisotropically. The crystallographic data and structure refinements are presented in Table 1.

Crystallographic data (excluding structure factors) for the structures in this paper have been deposited with the Cambridge Crystallographic Data Centre, CCDC, 12 Union Road, Cambridge CB21EZ, UK. Copies of the data can be obtained free of charge on quoting the depository numbers CCDC-890416 for **1** and CCDC-900724 for **2** (Fax: +44-1223-336-033; E-Mail: deposit@ccdc.cam.ac.uk, http://www.ccdc.cam.ac.uk).

Synthesis of {[Zn$_2$(BMB)(5-AIPA)$_2$]·2H$_2$O}$_n$ (1): A mixture of BMB (0.266 g, 1 mmol), 5-AIPA (0.181 g, 1 mmol), and Zn(NO$_3$)$_2$·6H$_2$O (0.149 g, 0.5 mmol) was dissolved in DMF/H$_2$O = 4:1 (10 mL). The mixture was stirred for about 30 min and THF (0.05 mL) was slowly added. The mixture was transferred to a 25 mL stainless steel reactor with Teflon liner and heated to 150 °C automatically. The temperature was kept at 150 °C for 4 d and cooled to room temperature at the rate of 5 K·h^{-1}. Colorless block crystals of **1** were obtained. Yield: 72 %. Elemental analysis: calcd: C 48.50; H 4.03; N 10.65 %; found: C 48.52; H 4.04; N 10.61 %. **IR** (KBr): ṽ = 3452 s, 3143 s, 1575 s, 1507 w, 1399 s, 1250 w, 1137 m, 1006 w, 962 w, 887 w, 781 m, 744 m, 670 w cm^{-1}.

Synthesis of [Zn(BMB)(5-NIPA)]$_n$ (2): The synthesis of **2** was similar to the above description for **1** except that 5-AIPA was replaced by 5-NIPA. Colorless block crystals of **2** were obtained. Yield: 77 %. Elemental analysis: calcd: C 52.24; H 3.87; N 12.96 %; found: C, 53.25; H, 3.82; N, 12.94 %. **IR** (KBr): ṽ = 3440 s, 3128 s, 1638 s, 1536 w, 1400 s, 1338 m, 1273 w, 1114 w, 1001 w, 923 w, 870 w, 725 m, 666 w cm^{-1}.

Supporting Information (see footnote on the first page of this article): TGA curves of compounds **1** and **2**. XRPD spectra of **1** and **2** at room temperature.

Acknowledgements

This work was supported by the Natural Scientific Research Foundation of Shaanxi Provincial Education Office (No. 11JK0590), the Natural Science Foundation of Shaanxi Province (No. 2009JZ001), the National Science Fund for Fostering Talents in Basic Science (No. J1210057), and the State Key Program of National Natural Science of China (No. 20931005).

References

[1] E. D. Bloch, D. Britt, C. Lee, C. J. Doonan, F. J. Uribe-Romo, H. Furukawa, J. R. Long, O. M. Yaghi, *J. Am. Chem. Soc.* **2010**, *132*, 14382–14384.
[2] N. Stock, S. Biswas, *Chem. Rev.* **2012**, *112*, 933–969.
[3] P. Pachfule, R. Das, P. Poddar, R. Banerjee, *Inorg. Chem.* **2011**, *50*, 3855–3865.
[4] X. H. Bu, W. Chen, W. F. Hou, M. Du, R. H. Zhang, F. Brisse, *Inorg. Chem.* **2002**, *41*, 3477–3482.
[5] J. S. Hu, Y. J. Shang, X. Q. Yao, L. Qin, Y. Z. Li, Z. J. Guo, H. G. Zheng, Z. L. Xue, *Cryst. Growth Des.* **2010**, *10*, 2676–2684.
[6] M. Ahmad, M. K. Sharma, R. Das, P. Poddar, P. K. Bharadwaj, *Cryst. Growth Des.* **2012**, *12*, 1571–1578.
[7] X. Xi, Y. Fang, T. Dong, Y. Cui, *Angew. Chem. Int. Ed.* **2010**, *49*, 1–6.
[8] E. W. Lee, Y. J. Kim, D. Y. Jung, *Inorg. Chem.* **2002**, *41*, 501–506.
[9] B. Xu, J. Lü, M. Cao, L. Han, R. Cao, *Inorg. Chem. Commun.* **2011**, *14*, 1237–1240.
[10] R. L. Sang, L. Xu, *Eur. J. Inorg. Chem.* **2010**, *31*, 4962–4968.
[11] X. L. Wang, Y. Q. Chen, Q. Gao, H. Y. Lin, G. C. Liu, J. X. Zhang, A. X. Tian, *Cryst. Growth Des.* **2010**, *10*, 2174–2184.
[12] H. Sun, W. Xie, S. Lv, Y. Xu, Y. Wu, Y. Zhou, Z. Ma, M. Fang, H. K. Liu, *Dalton Trans.* **2012**, *41*, 7590–7594.
[13] Z. H. Cui, S. S. Wang, X. G. Wang, D. Z. Gao, Y. Q. Sun, G. Y. Zhang, Y. Y. Xu, *Z. Anorg. Allg. Chem.* **2012**, *638*, 669–674.
[14] F. Dai, J. Dou, H. He, X. Zhao, D. Sun, *Inorg. Chem.* **2010**, *49*, 4117–4124.
[15] R. Sun, Y. Z. Li, J. Bai, Y. Pan, *Cryst. Growth Des.* **2007**, *7*, 890–894.

[16] T. F. Liu, J. Lv, C. B. Tian, M. N. Cao, Z. J. Lin, R. Cao, *Inorg. Chem.* **2011**, *50*, 2264–2271.

[17] I. C. Hwang, R. P. Chandran, N. J. Singh, M. Khandelwal, T. D. Thangadurai, J. W. Lee, J. A. Chang, K. S. Kim, *Inorg. Chem.* **2006**, *45*, 8062–8069.

[18] F. H. Zhao, Y. X. Che, J. M. Zheng, *CrystEngComm* DOI: 10.1039/c2ce25911g.

[19] L. Dobrzanska, H. G. Raubenheimer, L. J. Barbour, *Chem. Commun.* **2005**, *40*, 5050–5052.

[20] Y. Gao, B. Twamley, J. N. M. Shreeve, *Inorg. Chem.* **2006**, *45*, 1150–1155.

[21] X. Y. Huang, K. F. Yue, J. C. Jin, J. Q. Liu, C. J. Wang, Y. Y. Wang, Q. Z. Shi, *Inorg. Chem. Commun.* **2010**, *13*, 338–341.

[22] L. L. Xu, J. G. Cheng, K. F. Yue, Y. L. Liu, C. J. Wang, Y. Y. Wang, *Z. Anorg. Allg. Chem.* **2012**, *638*, 366–371.

[23] Y. L. Liu, K. F. Yue, B. H. Shan, L. L. Xu, C. J. Wang, Y. Y. Wang, *Inorg. Chem. Commun.* **2012**, *15*, 30–33.

[24] C. Xu, Q. Guo, X. Wang, H. Hou, Y. Fan, *Cryst. Growth Des.* **2011**, *11*, 1869–1879.

[25] W. L. Leong, J. J. Vittal, *Chem. Rev.* **2011**, *111*, 688–764.

[26] J. Tao, X. Yin, Z. B. Wei, R. B. Huang, L. S. Zheng, *Eur. J. Inorg. Chem.* **2004**, 125–133.

[27] H. Ren, T. Y. Song, J. N. Xu, S. B. Jing, Y. Yu, P. Zhang, L. R. Zhang, *Cryst. Growth Des.* **2009**, *9*, 105–112.

[28] X. Li, R. Cao, W. Bi, Y. Wang, Y. Wang, X. Li, Z. Guo, *Cryst. Growth Des.* **2005**, *5*, 1651–1656.

[29] X. C. Chai, Y. F. Zhao, Q. J. Gong, Y. P. Liang, H. H. Zhang, Y. P. Chen, *Z. Anorg. Allg. Chem.* **2012**, *638*, 641–647.

[30] Y. X. Hu, H. B. Ma, B. Zheng, W. W. Zhang, S. Xiang, L. Zhai, L. F. Wang, B. Chen, X. M. Ren, J. Bai, *Inorg. Chem.* **2012**, *51*, 7066–7074.

[31] B. Liu, L. Y. Pang, L. Hou, Y. Y. Wang, Y. Zhang, Q. Z. Shi, *CrystEngComm* DOI: 10.1039/C2CE26058A.

[32] G. M. Sheldrick, *SHELXTL*, Version 6.10, Bruker Analytical X-ray Systems, Madison, WI, **2001**

Received: July 21, 2012
Published Online: November 9, 2012